Supporting Information

Fluorenyl phenolphthalein groups containing multi-block copolymer membrane for alkaline fuel cells

Ajay K. Singh,[a,c] Ravi P. Pandey, [a,b] Vinod K. Shahi [a,b]*

[a] *Electro-Membrane Processes Division,*
CSIR-Central Salt and Marine Chemicals Research Institute (CSIR-CSMCRI),
Council of Scientific & Industrial Research (CSIR),
Gijubhai Badheka Marg, Bhavnagar- 364 002, (Gujarat), INDIA
Fax: +91-0278-2566970; E-mail: vkshahi@csmcri.org; vinodshahi1@yahoo.com
[b] *Academy of Scientific and Innovative Research,*
CSIR-Central Salt and Marine Chemicals Research Institute (CSIR-CSMCRI),
Council of Scientific & Industrial Research (CSIR), Bhavnagar- 364 002, (Gujarat), INDIA
[c]*Department of Chemical Engineering, POSTECH (Pohang University of Science and Technology), Pohang, Korea 790-784*

S1. Instrumental Characterization of the membranes: FTIR spectra of dried membrane samples were obtained by Spectrum GX series 49387 spectrometer in the range of 4000-450 cm^{-1}. The IR spectrum for a synthesized intermediate was obtained by the KBr pellet method. ^{1}H, and ^{13}C were used to characterize the synthesized material recorded by an NMR spectrometer (Bruker 500 MHz) in a D_2O and d_6-DMSO solvent. The thermal degradation processes and stabilities of the membranes were investigated using a thermogravimetric analyzer (Mettler Toledo TGA/SDTA851 with *Star* software) under a nitrogen atmosphere with a heating rate of 10 °C/min from 30 to 800 °C. Differential scanning calorimetry (DSC) measurements were carried out in a temperature range of 30-300 °C with a heating rate of 5 °C/min. The dynamic mechanical stabilities of membranes were evaluated by using a Mettler Toledo dynamic mechanical analyzer 861 instruments with Star software under nitrogen with a heating rate of 10 °C/min from 30 to 410 °C. For scanning electron microscopy (SEM), gold sputter coating were carried out on desired membrane samples at pressure ranging in between 1 and 0.1 Pa. Sample was loaded in the machine, which was operated at 10^{-2} to 10^{-3} Pa with EHT 15.00 kv with 300 V collector bias using Leo microscope SEMs were recorded. The optical densities of microbial

solutions were evaluated by using a VARIAN 50 bio UV-Vis spectrophotometer instruments. Refractive index was obtained by using a digital refractometer (Mettler Toledo RE40D refractometer). Gel permeation chromatography (GPC, Waters 2695) equipped with Styragel hr 0.5, hr 4E, and hr 5 columns with reflective index detector. Dynamic light scattering measurements (DLS) were performed at 298.15 K on a Zetasizer Nano ZS light scattering apparatus (Malvern Instruments, U.K.) with a He_Ne laser (633 nm, 4Mw). Polymeric solutions of varying concentrations were filtered directly into a quartz cell using a membrane filter of 0.45 μm pore size. Prior to measurements, the quartz cell was rinsed several times with filtered water and then filled with filtered sample solutions. The temperature of the measurements was controlled to an accuracy of ±0.1 K.

S2. Water uptake and methanol uptake measurements: The membrane swelling properties were obtained in term of weight fraction of water uptake. For the determination of weight fraction of water, the membrane was immersed in distilled water for 24 h and weight of wet membrane was recorded after removing surfacial water. Then the wet membranes were dried under vacuum at 60 °C until to get a constant weight and thus dry weight of the membranes was recorded. The water uptake (φ_w) of the membranes was determined using the following equation:

$$Water\,uptake\,(\varphi_w,\%) = \frac{W_{wet} - W_{dry}}{W_{dry}}\ X\ 100$$

Where, W_{wet} and W_{dry} are the masses of the membrane under wet and dry conditions.

Similarly, methanol uptake (φ_m) was also measured.

S3. Hydrolytic stabilities: For hydrolytic stability test, a small piece of membrane was boiled in water for 500 h at 140 °C in a pressurized closed vial.[1-3] The stability was evaluated by weight loss observed in membrane after stability evaluation and appearance of the test samples.

S4. Ion-exchange capacity (IEC) measurements: IEC, defined as mequiv.(OH−)/g of dry membrane was determined by standard back-titration technique. The membrane was equilibrated in 1.0 M NaOH solution to convert into OH^- form and washed with distilled water to remove last trace of base. Thus hydroxyl form membranes were equilibrated in 50 ml of 0.1M NaCl solution for 24 h. The IEC was determined by acid–base titration of equilibrated NaCl solution.[4]

S5. Counter ion transport number measurements: Counter ion transport number in the membrane phase was obtained by potential measurements using TMS (Teorell, Meyer and Sievers) approach.[6] Experimental cell used for membrane potential measurements, had two compartments separated by a circular piece of membrane (7.0 cm^2) as reported previously.[6] For the minimization of boundary layer both compartments were vigorously stirred by a magnetic stirrer and the potential aroused across the membrane was recorded with the help of a multimeter using saturated calomel electrodes with salt bridge. For membrane potential measurements, the relationship between electrolyte concentrations of the higher (C_1) and the lower side (C_2) was taken as follows: C1/C2 = 10, $\Delta C/C_S = (C_1 - C_2)/[(C_1 + C_2)/2]$.

S6. Membrane conductivity studies: Conductivity of anion exchange membrane was measured by four-probe Ac impedance spectroscopy using a potentiostat/galvanostat frequency response analyzer (Auto Lab, Model PGSTAT 30). Prior to measurement, the membrane samples were soaked in deionized (DI) water for 24 h and rinsed repeatedly to remove the last trace of free acid or base. The membranes were mounted between two platinum electrodes (4.0 cm^2), which were then placed in DI water. Direct current (DC) and sinusoidal alternating currents (AC) were

supplied to the respective electrodes for recording the frequency at a scanning rate of 1 mA s within a frequency range 10^6 to 1 Hz. The spectrum of the blank short-circuited cell was also collected and this data was subtracted (as a series circuit) from each of the recorded spectra of the membranes to eliminate cell and wiring resistances and inductances. The corrected spectra were viewed as complex impedance plots with the imaginary component of Z'' on the y-axis and the real component of Z' on the x-axis (Z=Z' −iZ''); the ionic resistance of each membrane was estimated to be the intersection of the x-axis with the extrapolation of the low frequency linear component of each plot. The membrane resistances were obtained from Nyquist plots. The hydroxyl ion (OH^-) conductivity (k^m) was calculated by following equation:

$$k^m\ (S/cm) = \frac{L(cm)}{[R(\Omega)\,x\,A(cm^2)} \qquad (3)$$

Where L is the distance between the electrodes, R is the resistance of the membrane, and A is the surface area of the membrane.

S7. Methanol permeability

Methanol permeability of the composite membranes was determined in a diaphragm diffusion cell, consisting of two compartments (80 cm^3) separated by a vertical membrane with 20 cm^2 effective area. The membrane was clamped between both compartments, which were stirred during the experiments. Before the experiment, membranes were equilibrated in water-methanol mixture for 12 h. Initially, one compartment (A) contained 30 or 50% (v/v) methanol-water mixture while other (B) double distilled water. Methanol flux arises across the membrane as a result of concentration difference between two compartments. The increase in methanol concentration with time in compartment B was monitored by measuring the refractive index using a digital refractometer (Mettler Toledo RE40D refractometer). The methanol permeability (P) finally was obtained by the equation given below:

$$P = \frac{1}{AC_A(t-t_0)}\frac{C_{B(t)}}{V_B}l$$

where A is the effective membrane area, l the thickness of the membrane, $C_{B(t)}$ the methanol concentration in compartment B at time t, $C_A(t - t_0)$ the change in the methanol concentration in compartment A between time 0 and t, and V_B the volume of compartment B. All experiments were carried out at room temperature, and the uncertainty of the measured values was less than 2%.

References

1. B.P. Tripathi, V.K. Shahi, *J. Phys. Chem. B*, 2008, **112**, 15678.
2. B.P. Tripathi, V.K. Shahi, *ACS Appl. Mater. Interface,* 2009, **1**, 1002.
3. B.P. Tripathi, A. Saxena, V.K. Shahi, *J. Membr. Sci.,* 2008, **318**, 288.
4. J. Fang, P.K. Shen, *J. Membr. Sci.*, 2006, **285,** 317.
5. N. Lakshiminarayanaiah, Academic Press, New York, 1969.
6. R.K. Nagarale, G.S. Gohil, V.K. Shahi, R. Rangarajan, *J. Colloid Interface Sci.,* 2005 **287**, 198.

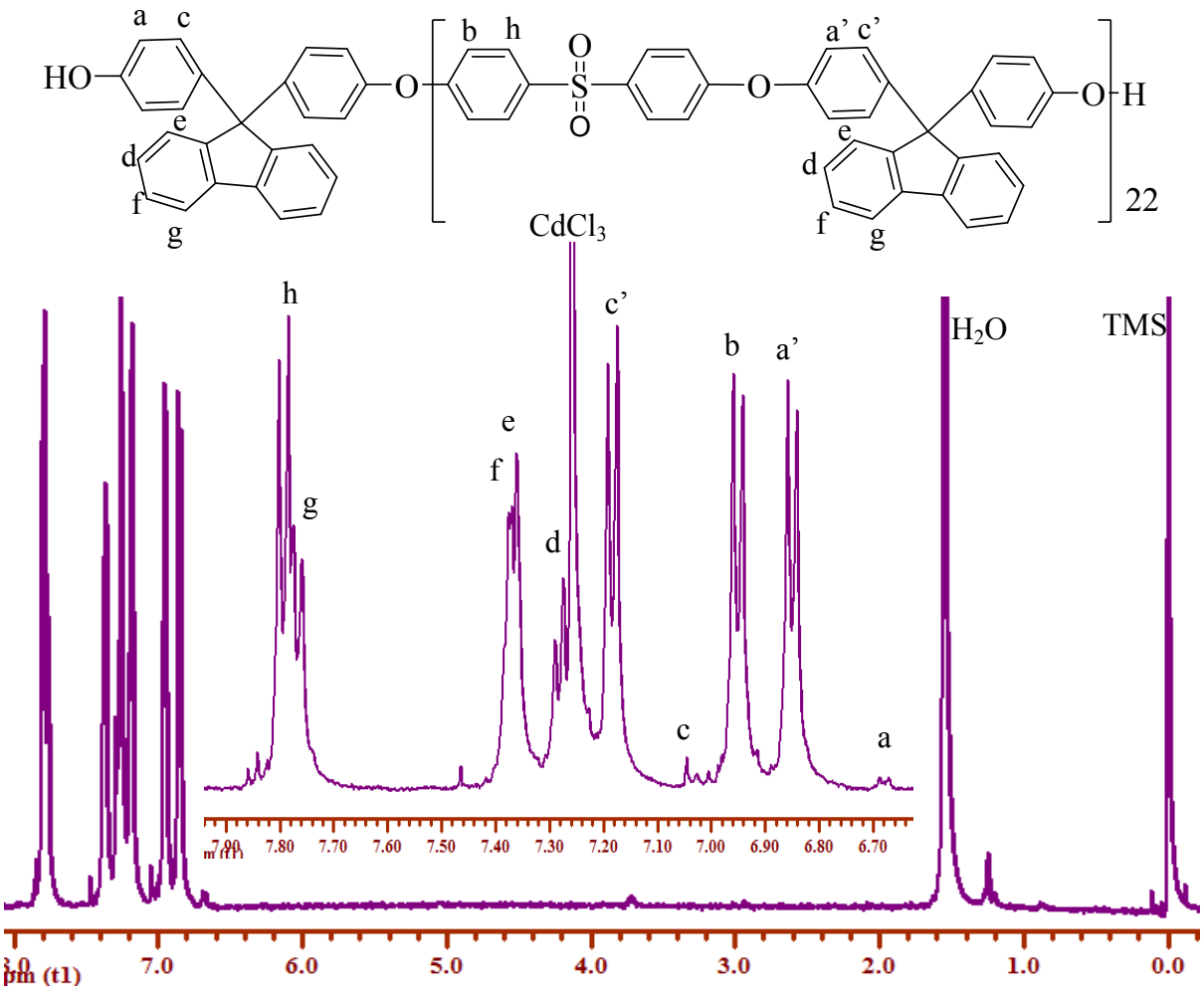

Fig. S1. ^{1}H NMR spectra of A_{22} oligomer.

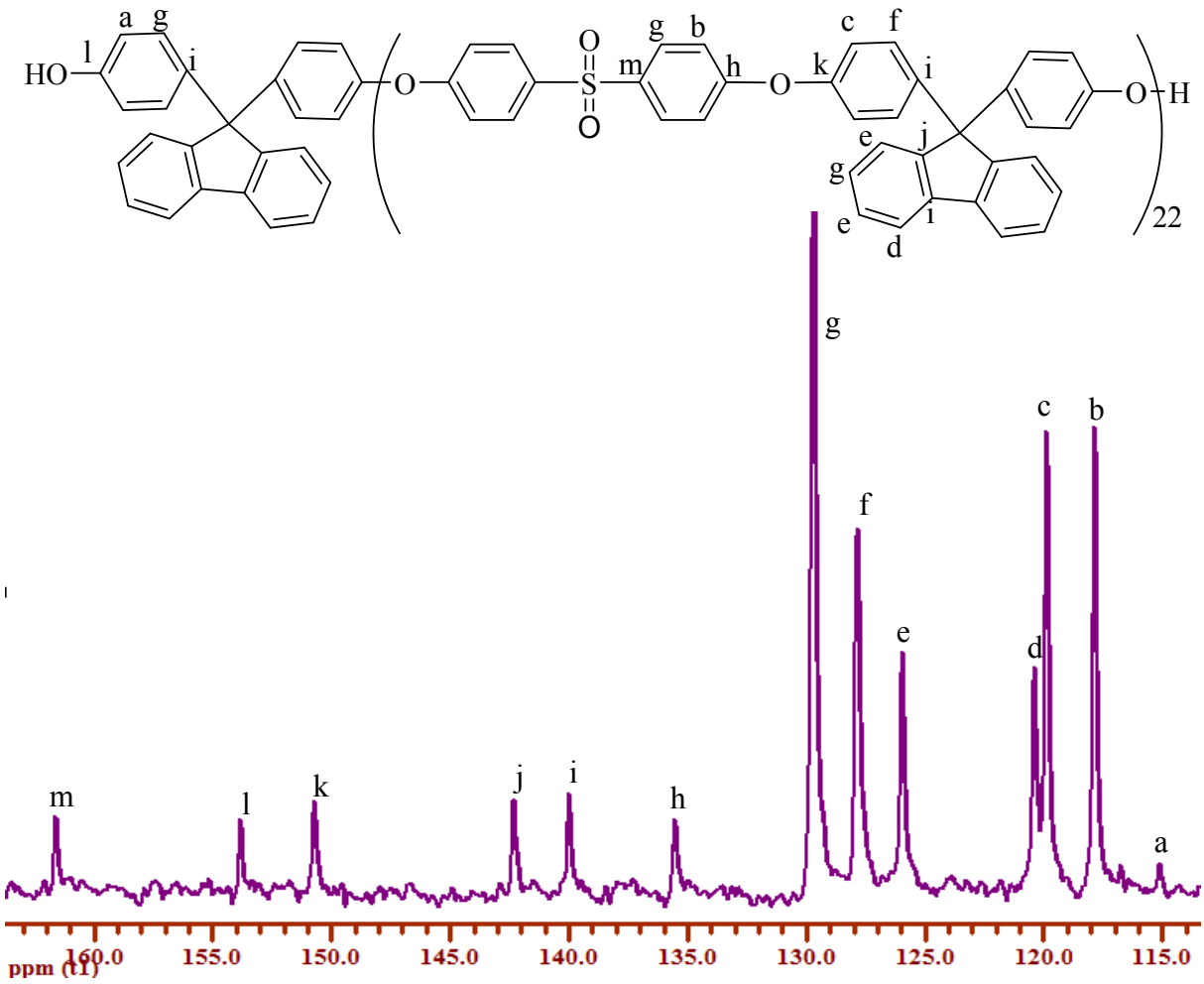

Fig. S2. ^{13}C NMR of A_{22} oligomer in deuterated chloroform.

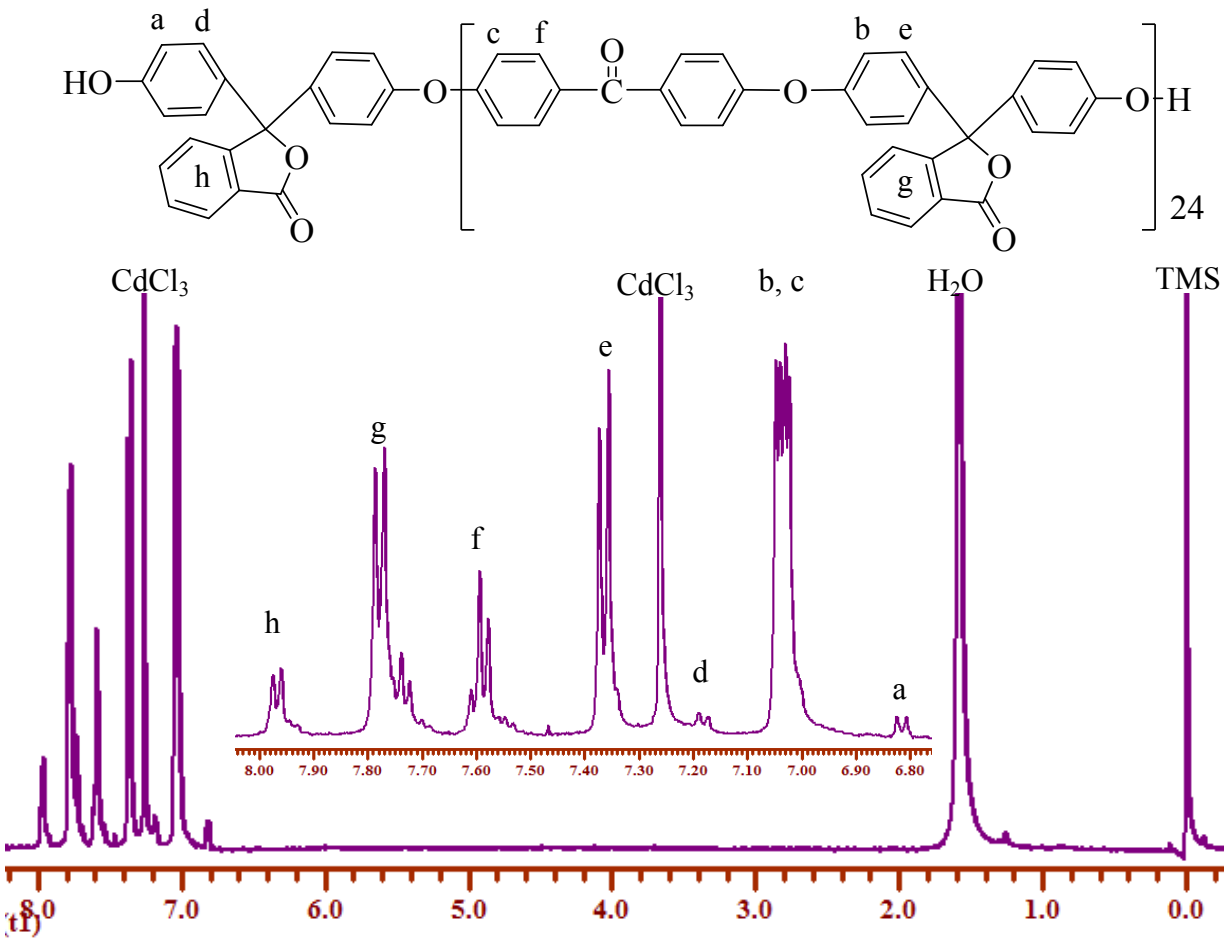

Fig. S3. ^{1}H NMR of B_{24} oligomer in deuterated chloroform.

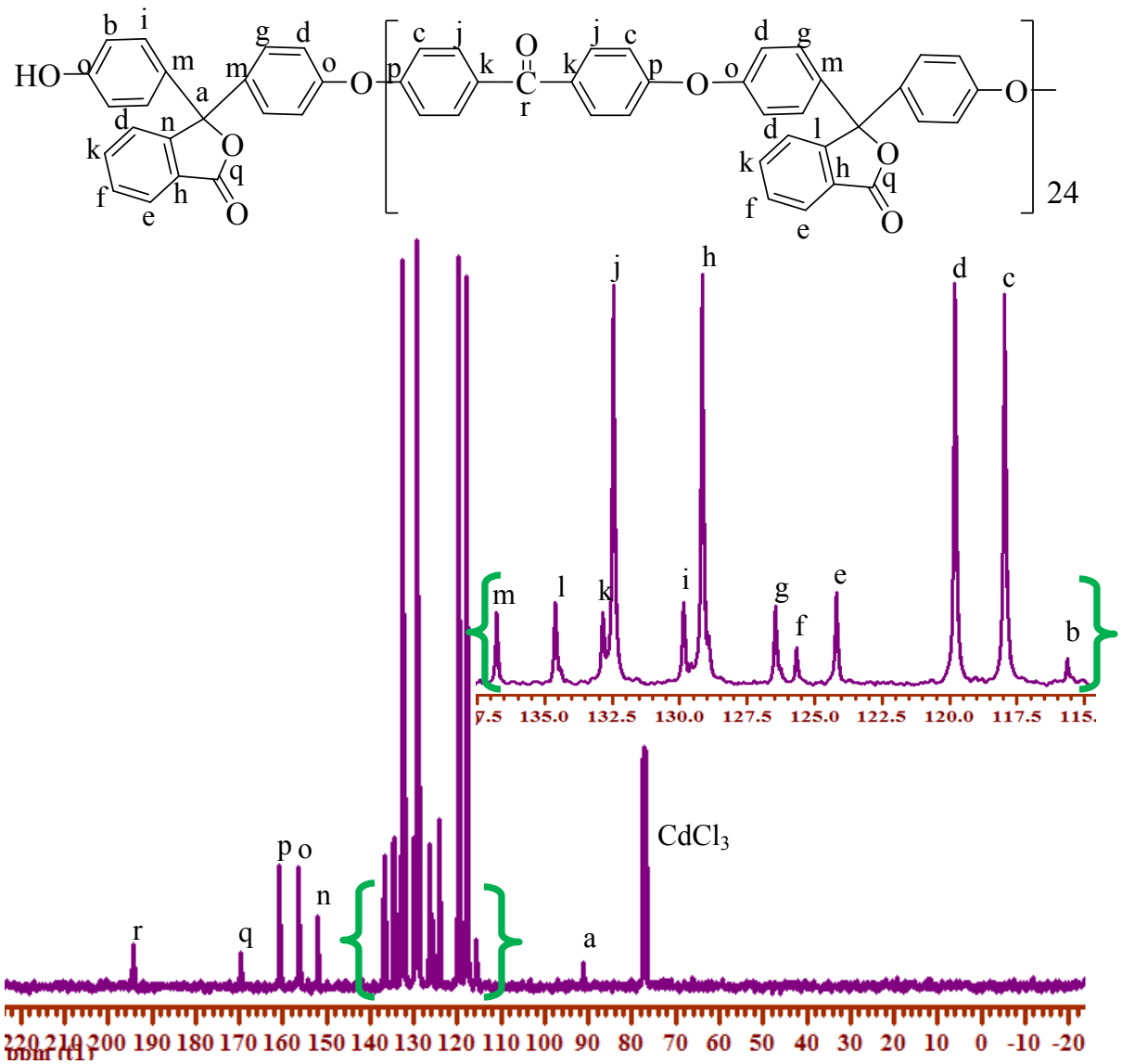

Fig. S4. ^{13}C NMR of B_{24} oligomer in deuterated chloroform.

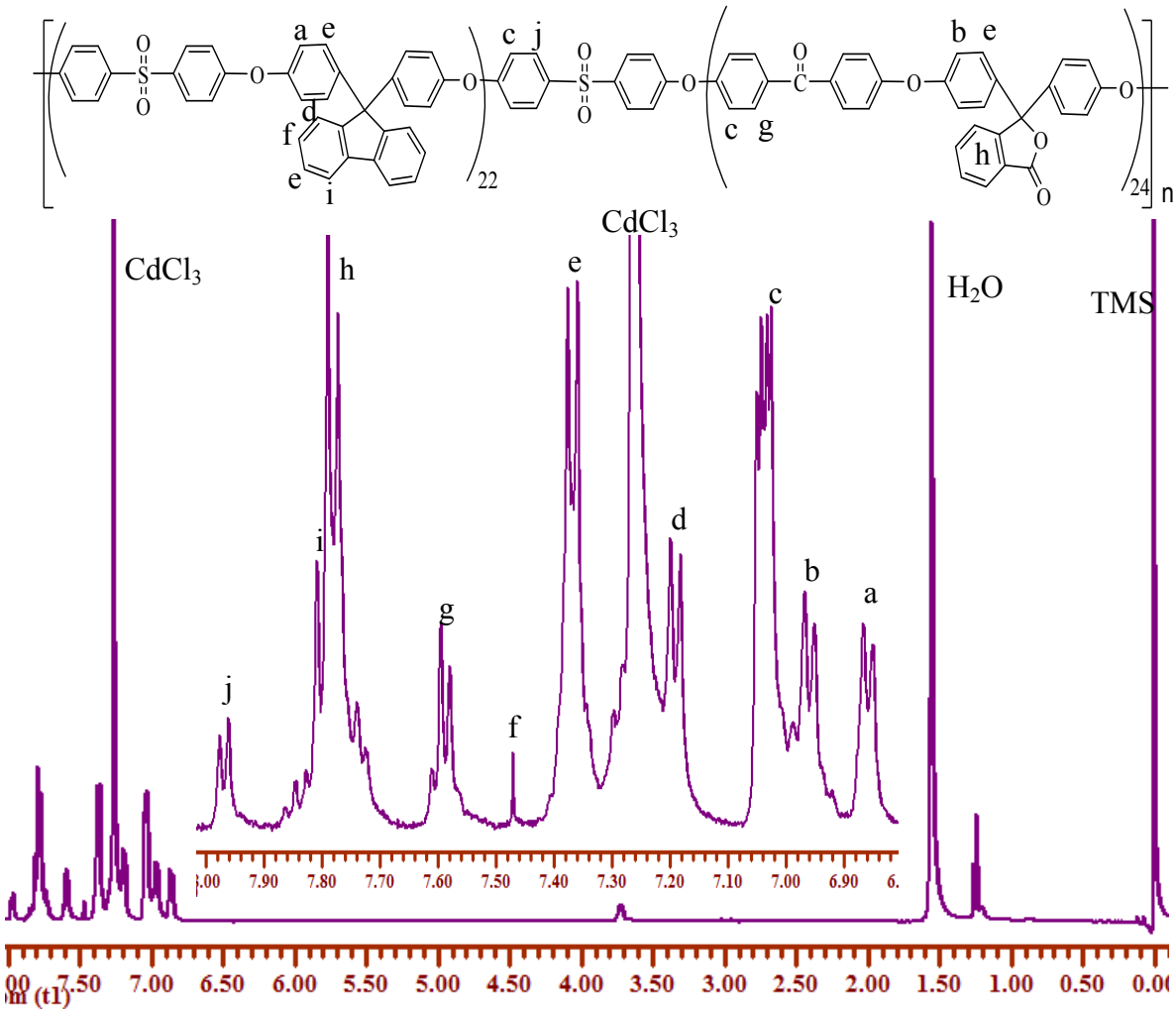

Fig. S5. ^{1}H NMR of multiblock copolymer (PE-$A_{22}B_{24}$) in deuterated chloroform.

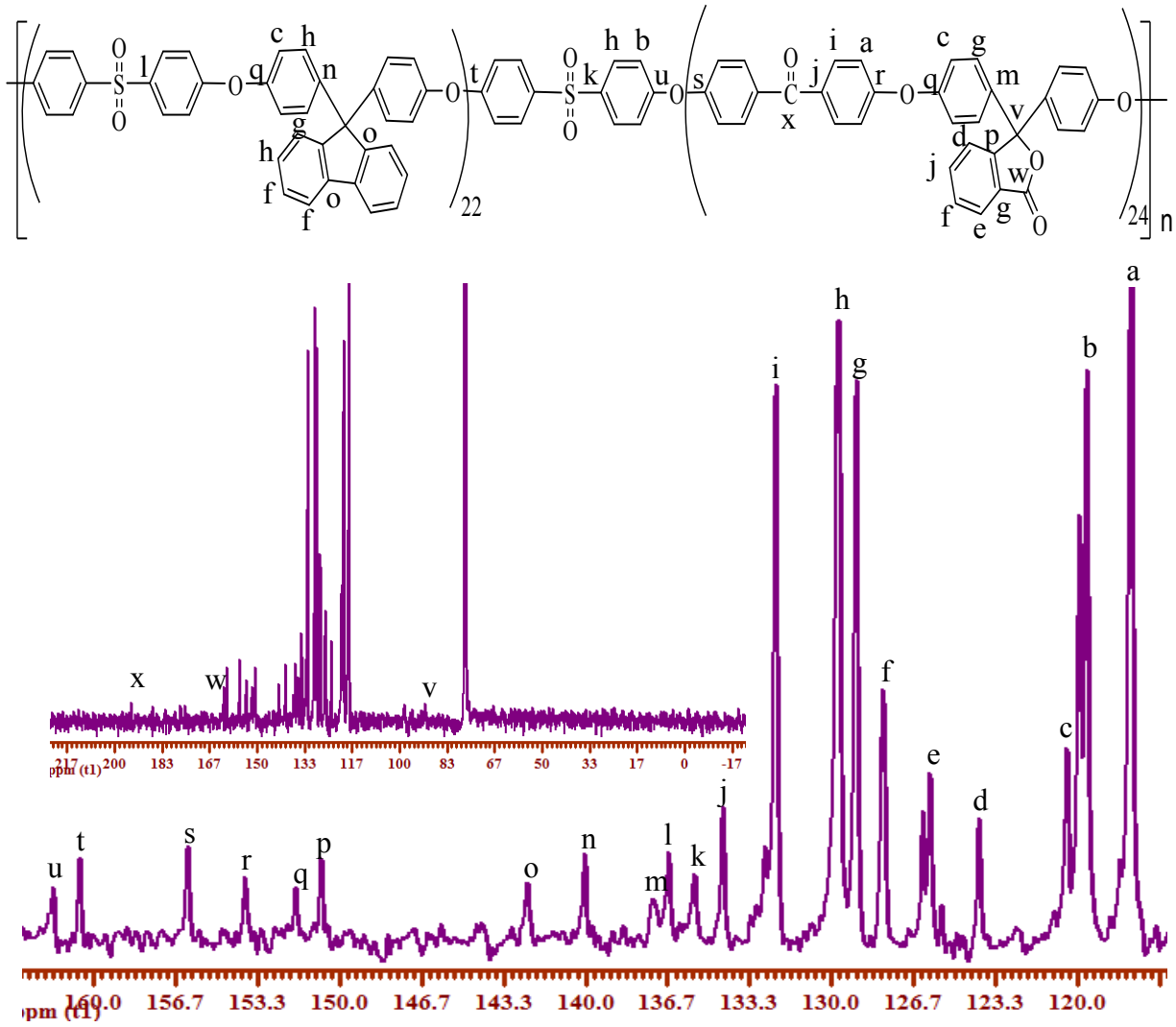

Fig. S6. ^{13}C NMR of multiblock copolymer (PE-$A_{22}B_{24}$) in deuterated chloroform.

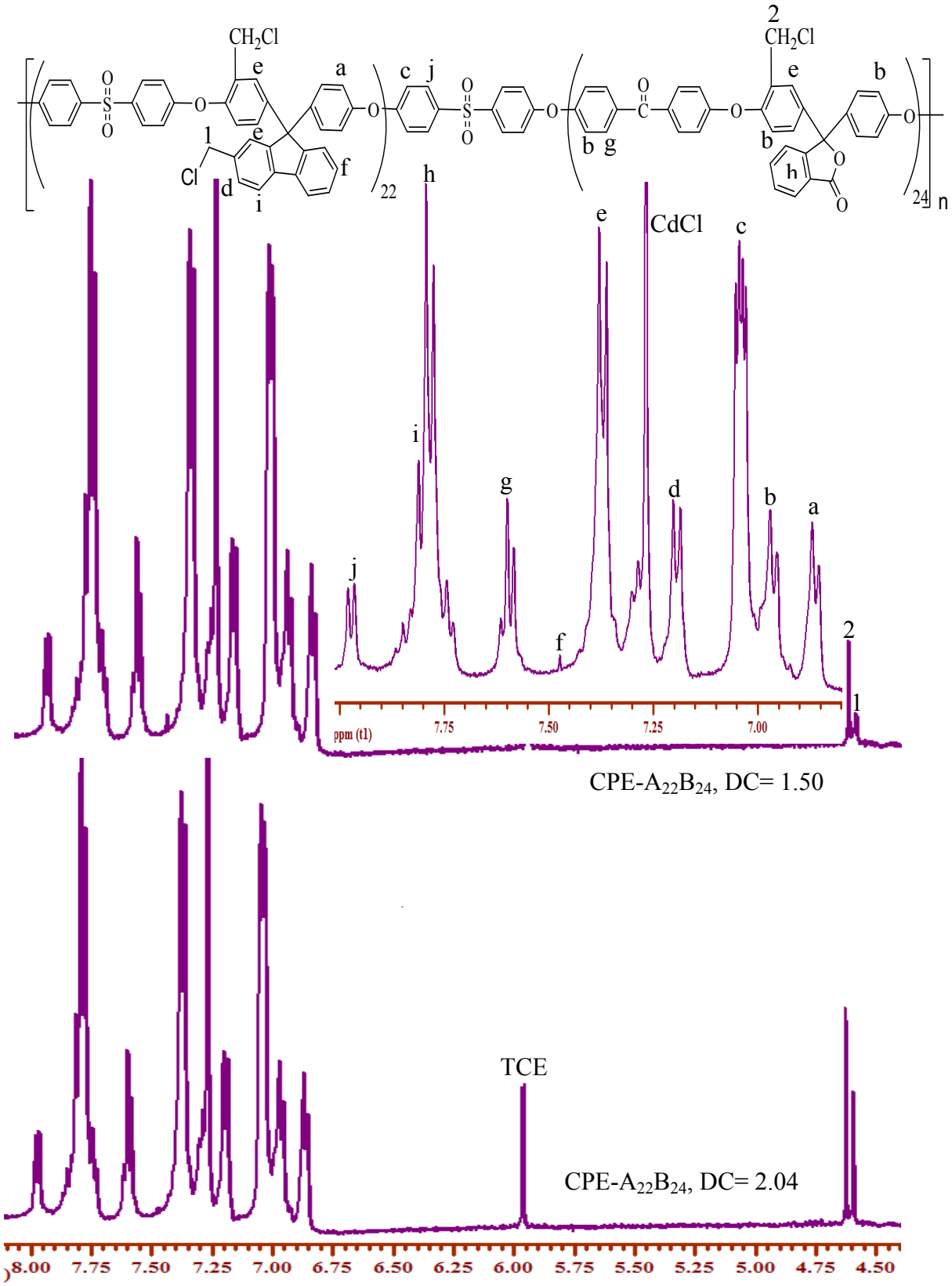

Fig. S7. ^{1}H NMR of chloromethyalted multiblock copolymer (CPE-$A_{22}B_{24}$) with different degree of chloromethylation in deuterated chloroform.

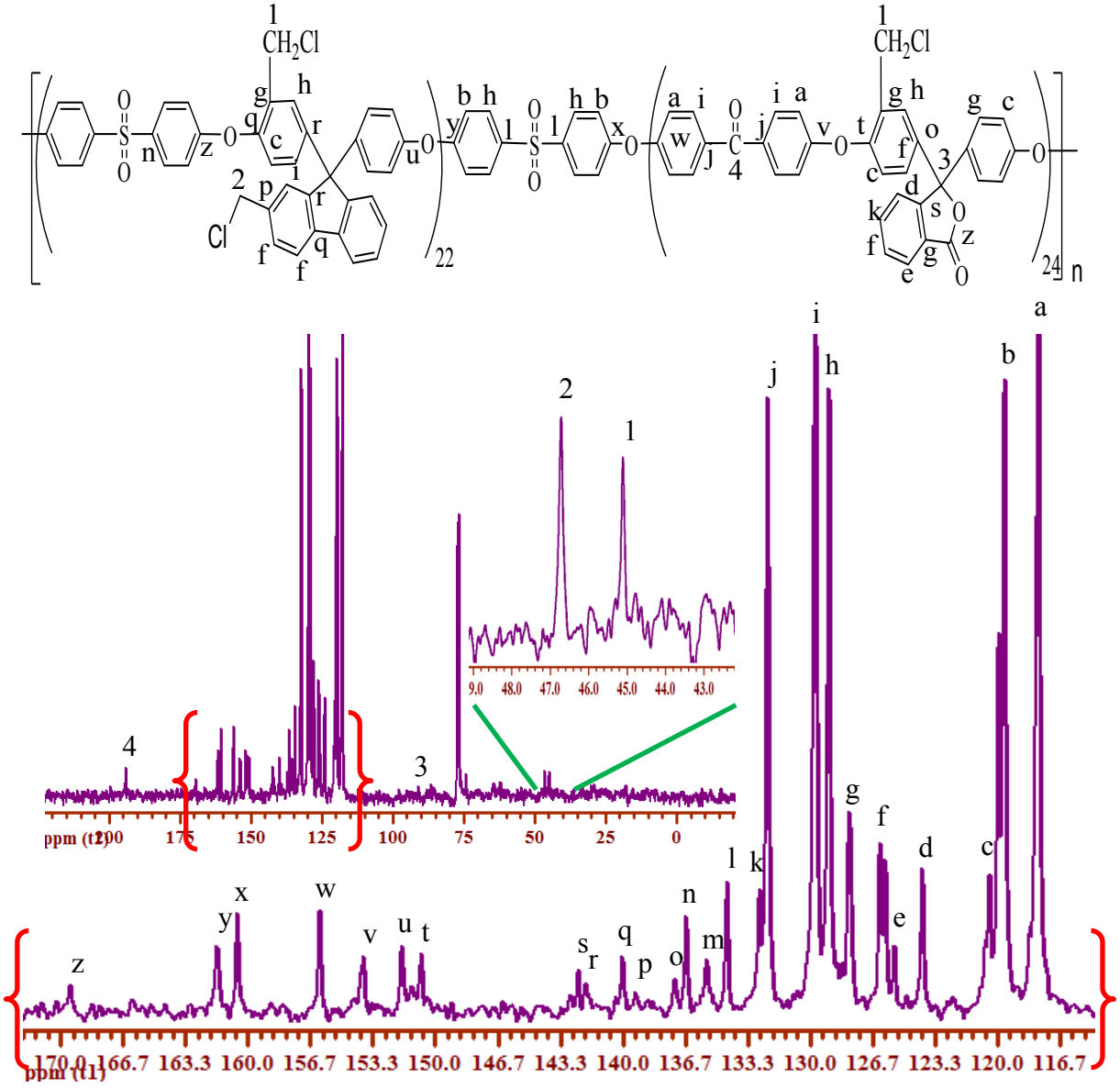

Fig. S8. ^{13}C NMR of chloromethyalted multiblock copolymer (CPE-$A_{22}B_{24}$) in deuterated chloroform.

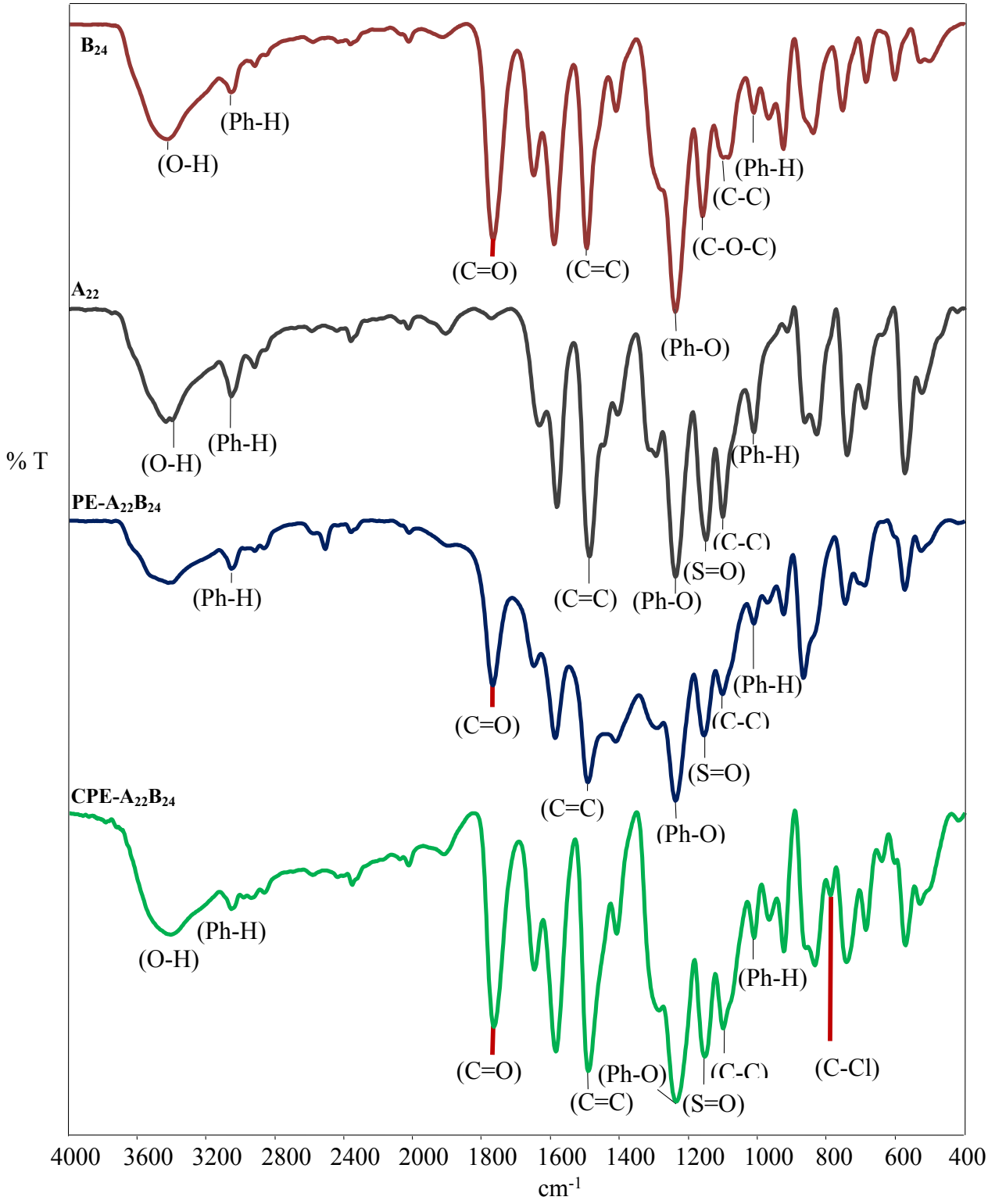

Fig. S9. FTIR spectra confirming the bonds formation of during block copolymerization and chloromethylation.

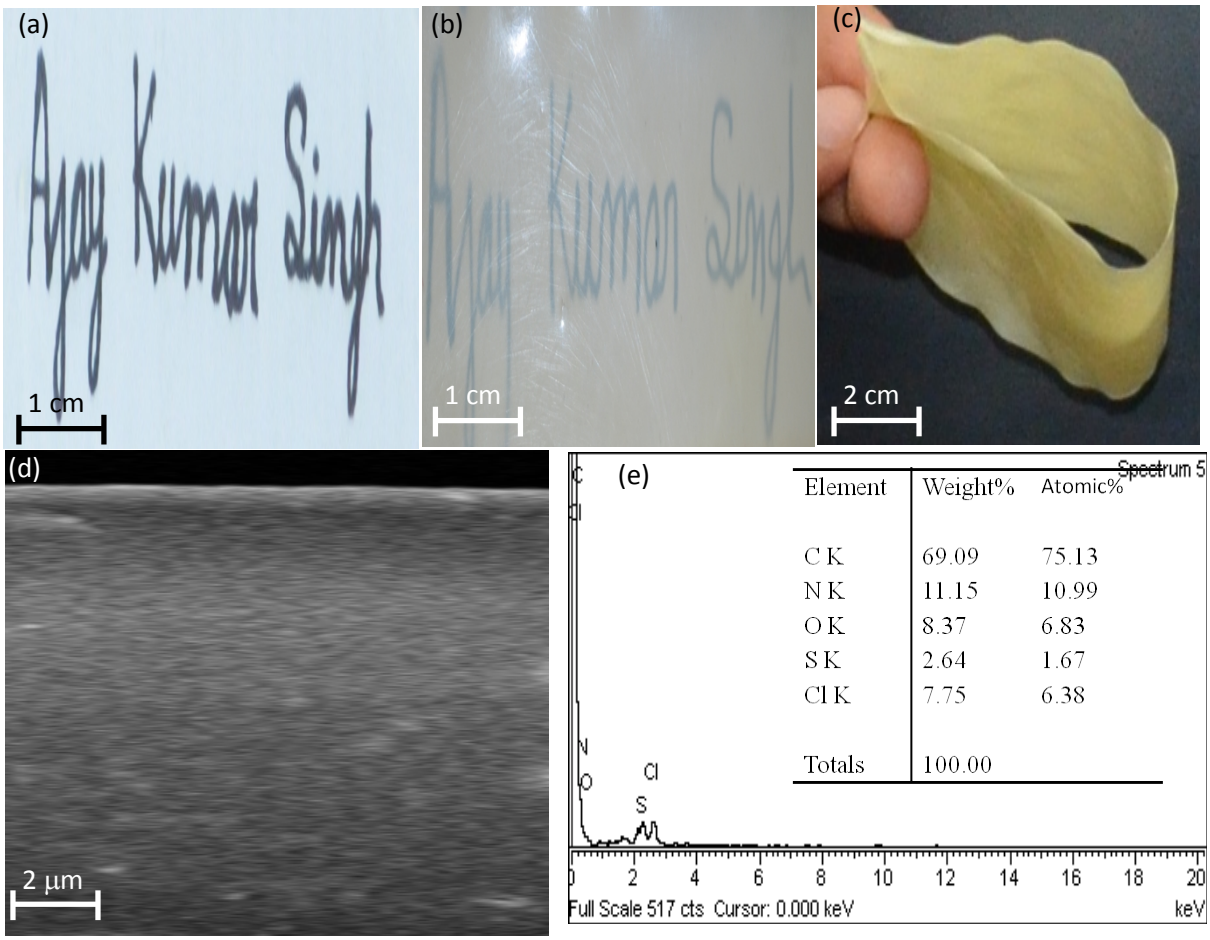

Fig. S10. Membrane morphology and EDX analysis: (a) optical image of transparent (colourless) CPE-$A_{22}B_{24}$ membrane; (b&c) transparent yellow coloured QPE-$A_{22}B_{24}$ membrane; (d) cross-sectional image of QPE-$A_{22}B_{24}$ membrane; (e) EDX data of QPE-$A_{22}B_{24}$ membrane.

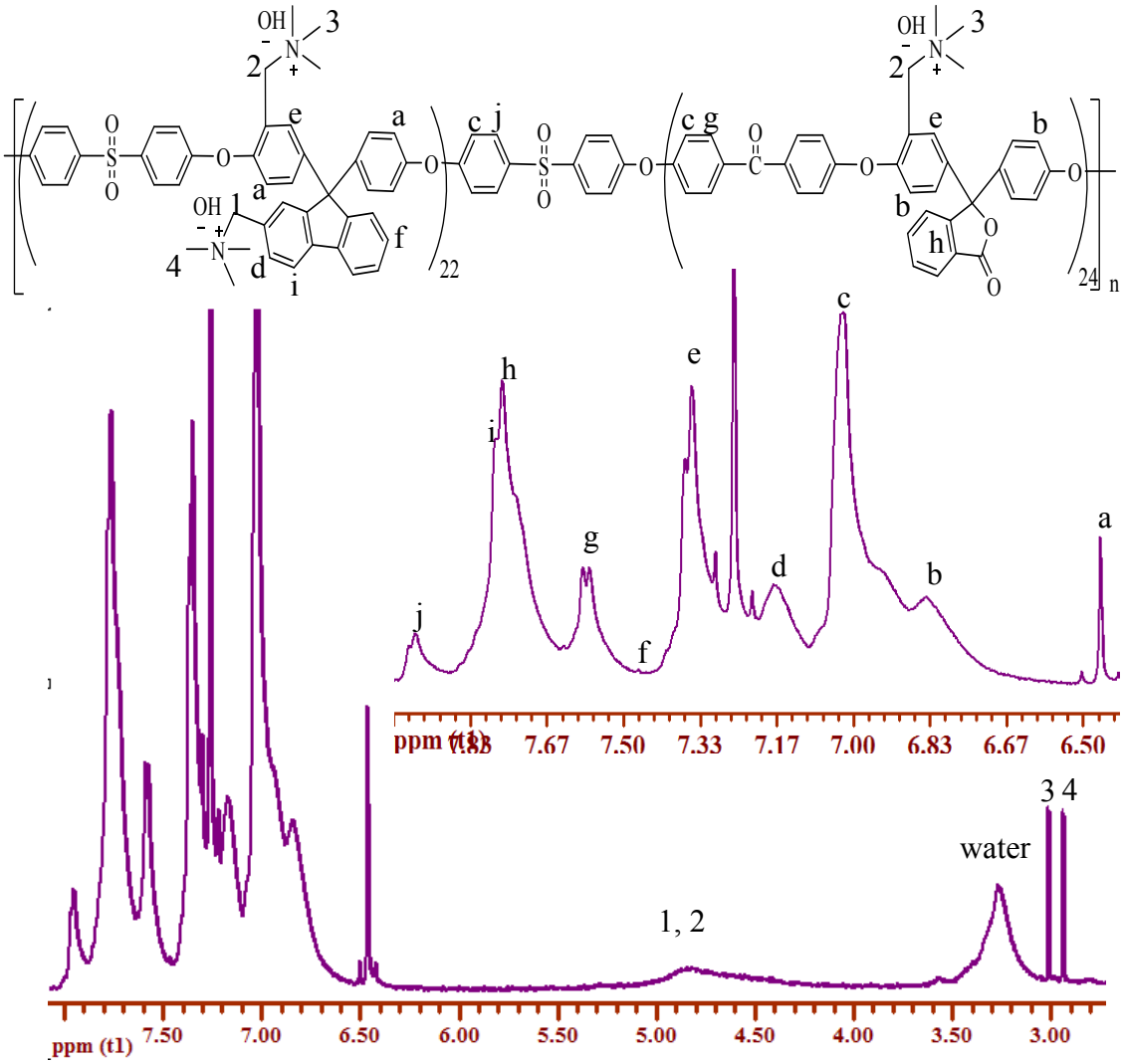

Fig. S11. ^{1}H NMR spectra of QPE-$A_{22}B_{24}$ (IEC = 0.95 meq/g).

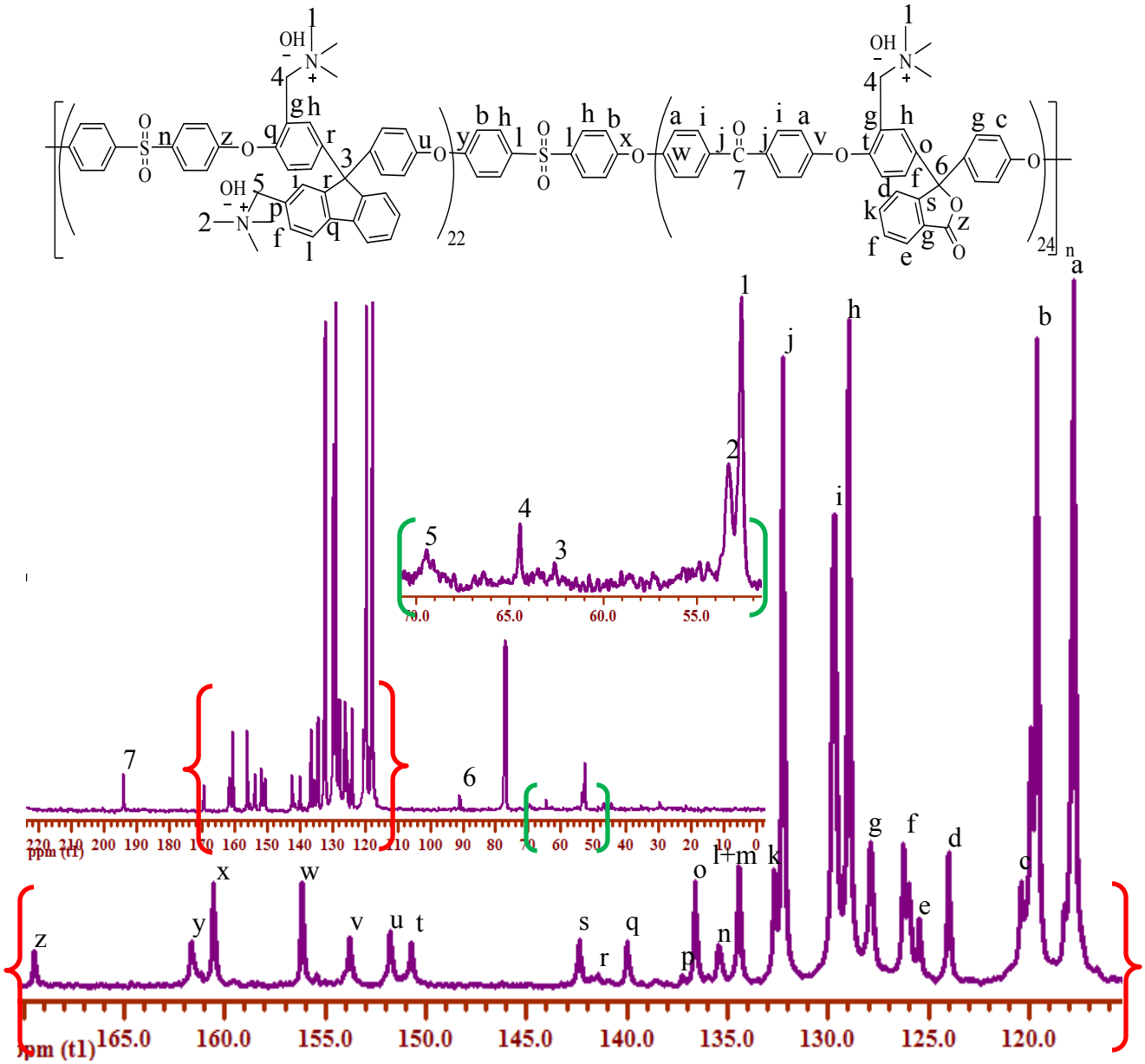

Fig. S12. ^{13}C NMR spectra of QPE-$A_{22}B_{24}$ (IEC = 0.95 meq/g).

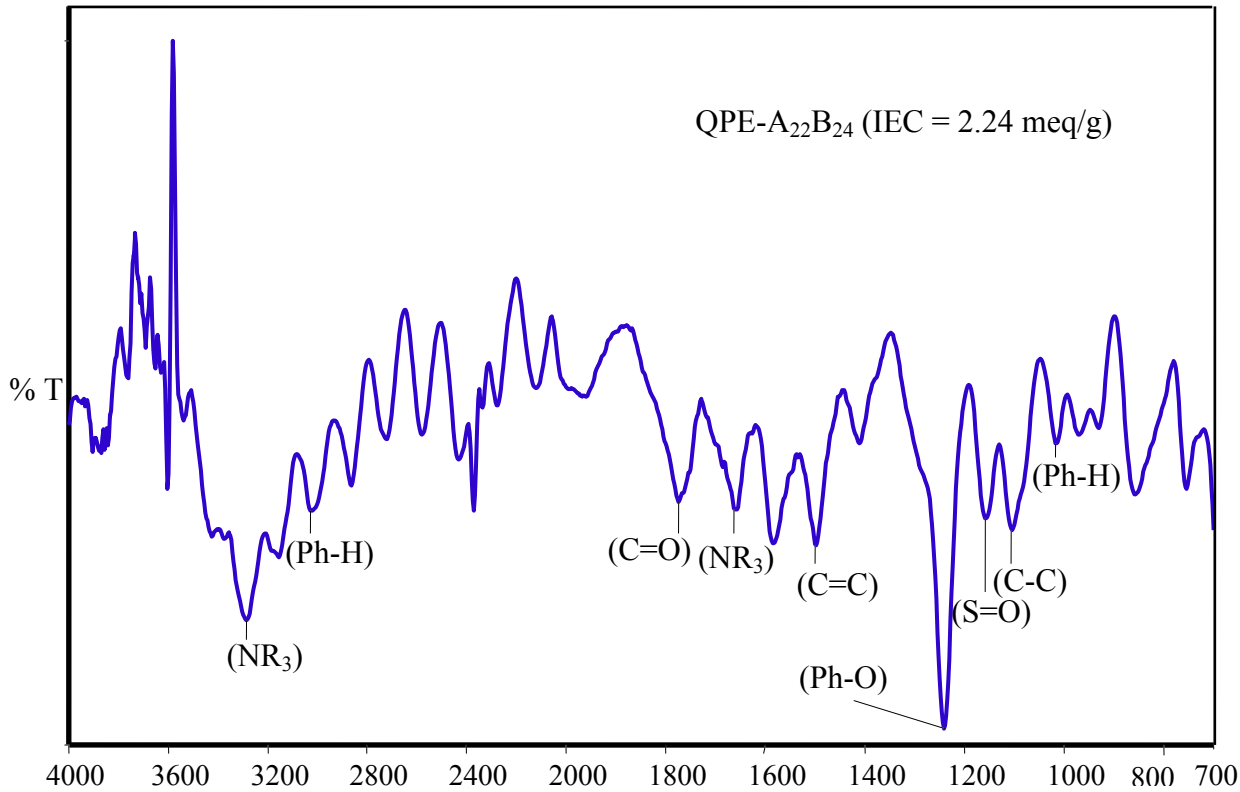

Fig. S13. Representative FT-ATR spectra of quternized membrane QPE-$A_{22}B_{24}$ (IEC = 2.24 meq/g).

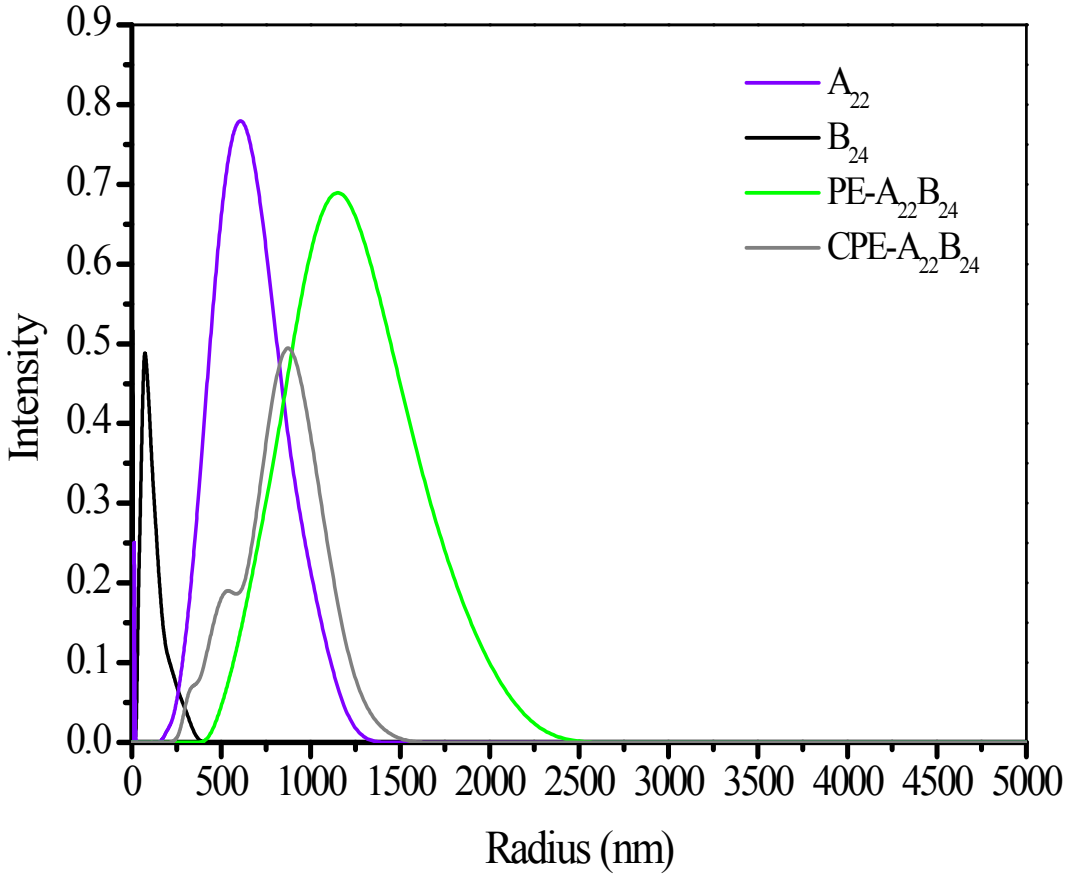

Fig. S14. DLS analysis of A_{22}, B_{24} oligomers, PE-$A_{22}B_{24}$ multiblock copolymer, and CPE-$A_{22}B_{24}$ chloromethylated copolymer at constant mole fraction (2×10^{-4}) in chloroform solvent.

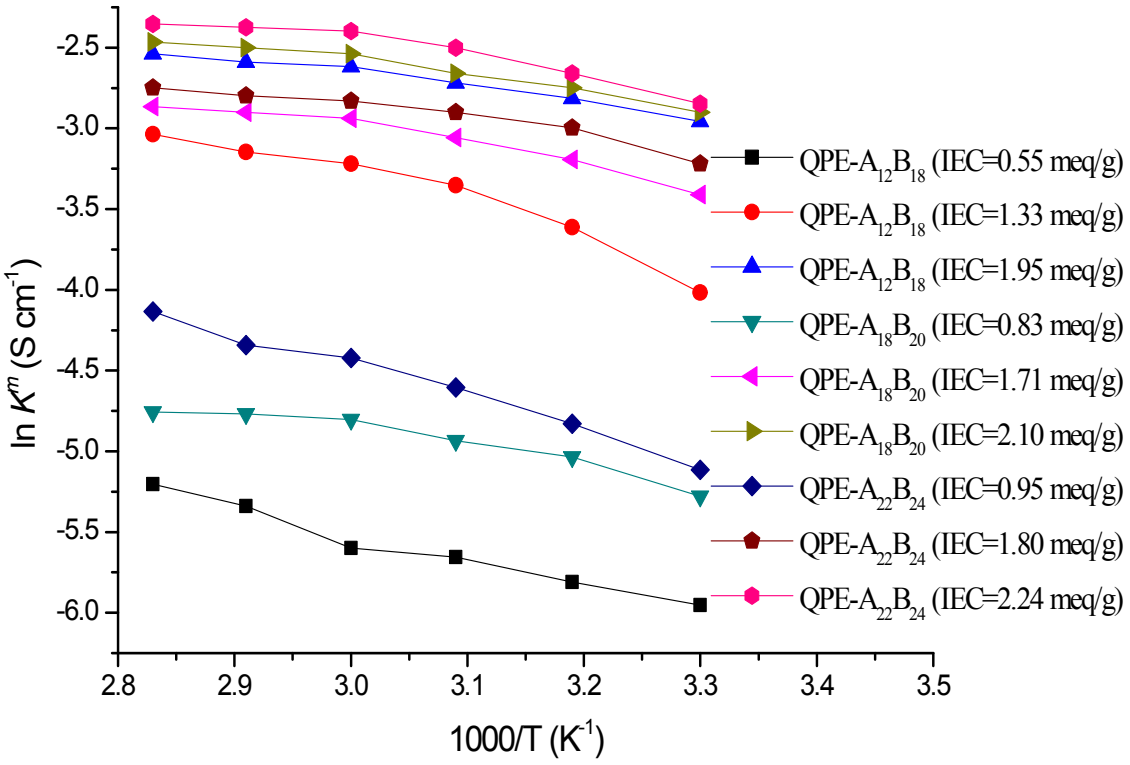

Fig. S15. Arrhenius plot in 100% RH environment for different anion-exchange membranes.

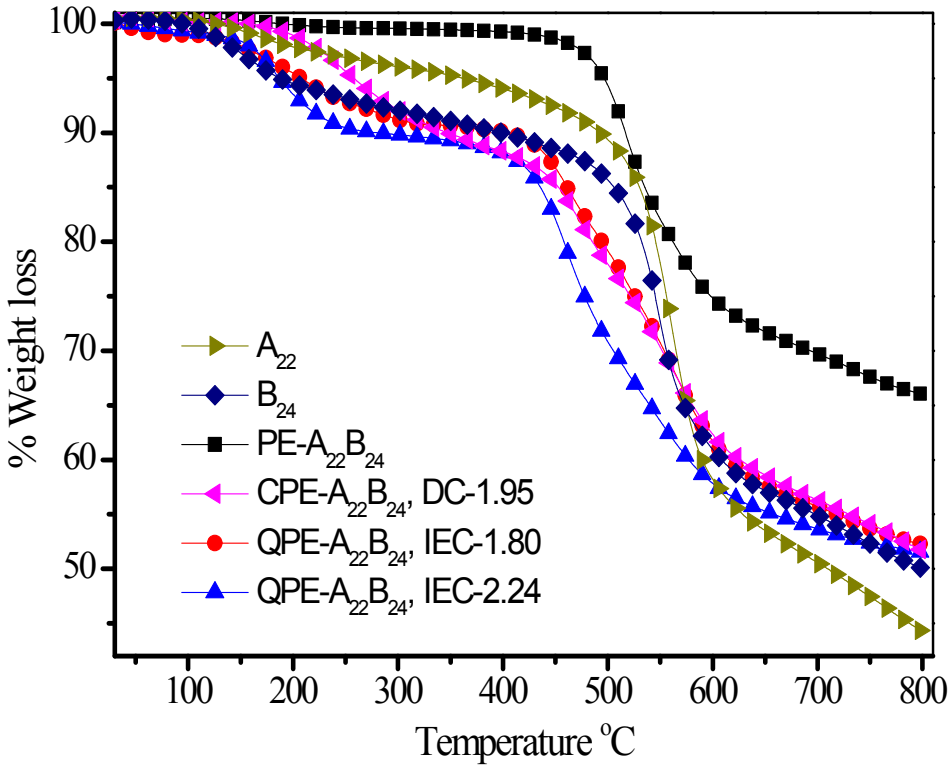

Fig. S16. Thermogravimetric analysis (TGA) of oligomer, multiblock copolymer, chlromethylated copolymer, and quaternized membrane.

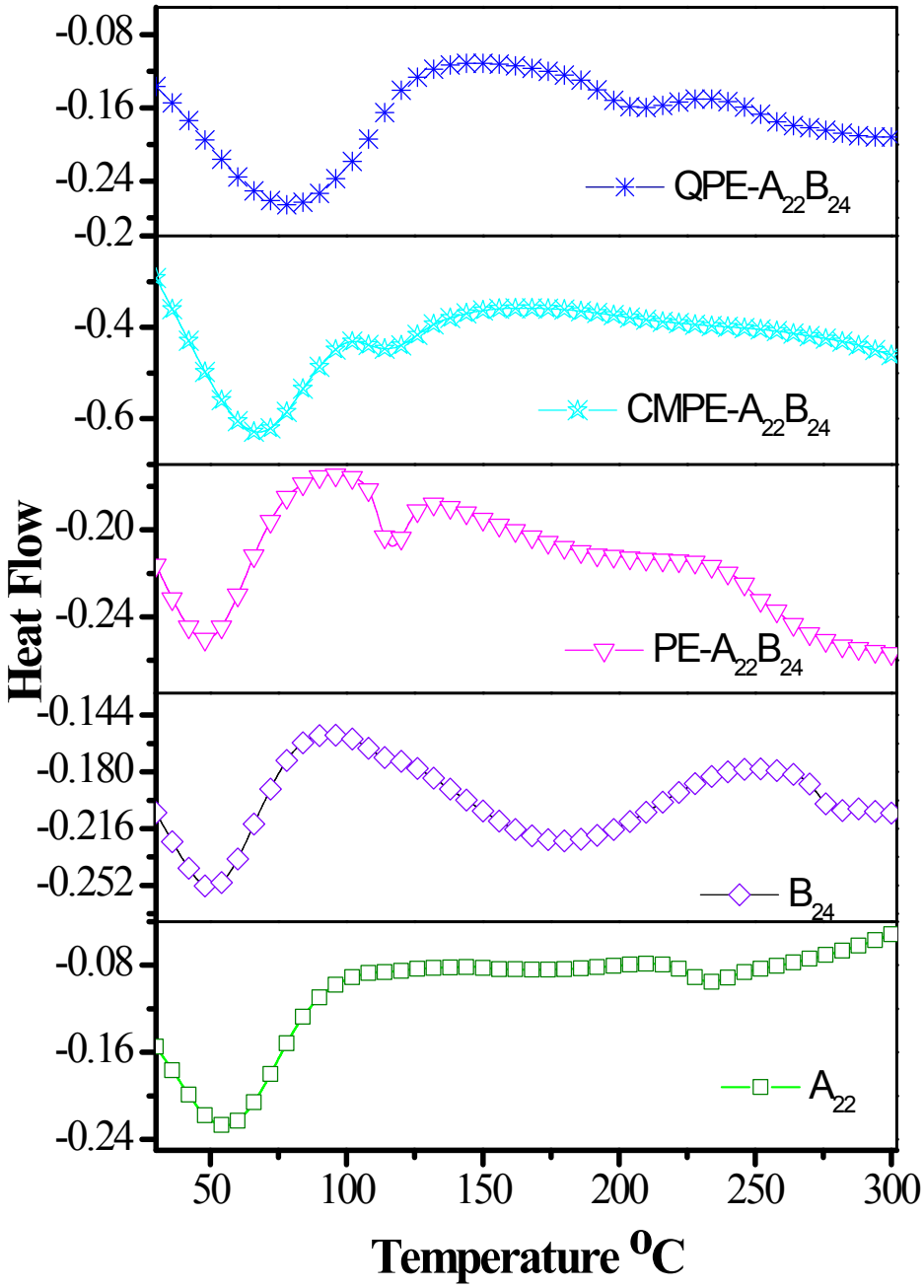

Fig. S17. DSC profile of hydrophilic oligomer, multiblock copolymer, chloromethylated and quaternized membrane.

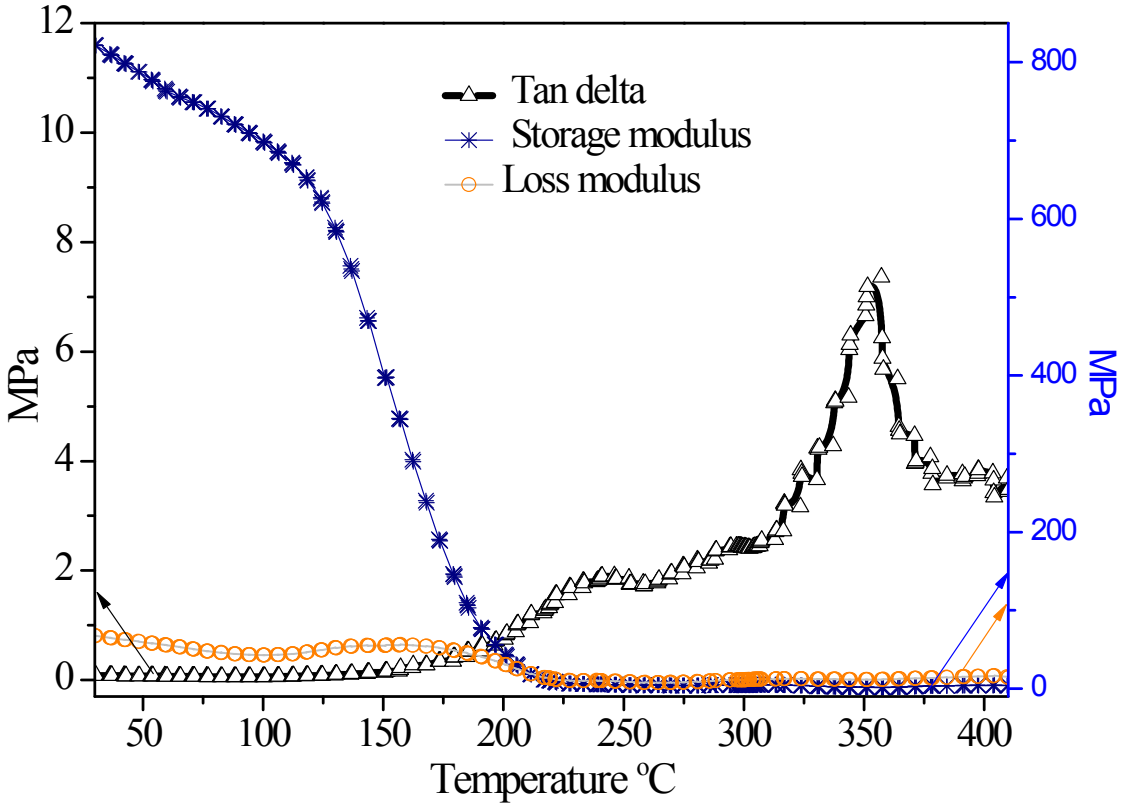

Fig. S18. Storage modulus, loss modulus, and tan delta vs temperature plots for quaternized membrane (QPE-$A_{22}B_{24}$, IEC = 2.24 meq/g).